NASA Technical Memorandum 106436
AIAA–94–0219

Optimization of Orifice Geometry for Cross-Flow Mixing in a Cylindrical Duct

W.A. Sowa, J.T. Kroll, and G.S. Samuelsen
UCI Combustion Laboratory
University of California
Irvine, California

and

J. D. Holdeman
National Aeronautics and Space Administration
Lewis Research Center
Cleveland, Ohio

Prepared for the
32nd Aerospace Sciences Meeting and Exhibit
sponsored by the American Institute of Aeronautics and Astronautics
Reno, Nevada, January 10–13, 1994

NASA

Optimization of Orifice Geometry for Cross-Flow Mixing in a Cylindrical Duct

W.A. Sowa†, J.T. Kroll‡, G.S. Samuelsen§
University of California
Irvine, CA

J. D. Holdeman††
NASA Lewis Research Center
Cleveland, Ohio

Abstract

Mixing of gaseous jets in a cross-flow has significant applications in engineering, one example of which is the dilution zone of a gas turbine combustor. Despite years of study, the design of jet injection in combustors is largely based on practical experience. A series of experiments was undertaken to delineate the optimal mixer orifice geometry. A cross-flow to core-flow momentum-flux ratio of 40 and a mass flow ratio of 2.5 were selected as representative of an advanced design. An experimental test matrix was designed around three variables: the number of orifices, the orifice aspect ratio (long-to-short dimension), and the orifice angle. A regression analysis was performed on the data to arrive at an interpolating equation that predicted the mixing performance of orifice geometry combinations within the range of the test matrix parameters. Results indicate that mixture uniformity is a non-linear function of the number of orifices, the orifice aspect ratio, and the orifice angle. Optimum mixing occurs when the asymptotic mean jet trajectories are in the range of $0.35 < r/R < 0.5$ (where r=0 is at the mixer wall) at $z/R = 1.0$. At the optimum number of orifices, the difference between shallow-angled slots with large aspect ratios and round holes is minimal and either approach will lead to good mixing performance. At the optimum number of orifices, it appears possible to have two local optimums where one corresponds to an aspect ratio of 1.0 and the other to a high aspect ratio.

List of Symbols

a	=	nodal area
A	=	total cross sectional area in the mixer
AR	=	orifice aspect ratio
C	=	constant, (e.g., see Eq. (1))
f	=	mixture fraction, (e.g., see Eq. (2))
$\bar{f}$	=	mean mixture fraction
h	=	orifice axial distance
J	=	momentum-flux ratio (jet/mainstream)
n	=	number of orifices
R	=	mixer radius
STD	=	area weighted standard deviation, (e.g., see Eq. (3))
T	=	gas temperature
x	=	regression model term
z	=	axial distance
α	=	orifice angle, 0=long axis aligned with flow

Introduction

Mixing of air jets into a cross flow is a fundamental part of gas turbine engine technology. Combustor efficiency, exit plane temperature pattern factor and effluent gas composition are strongly affected by the quality of the air jet-combustor gas mixing that is achieved. Because a significant amount of the combustion air is injected via jets through the side-wall, optimization of the combustor must consider wall orifice distribution, orifice size, jet penetration characteristics, and local enthalpy levels due to the jet mixing characteristics. Most of the important combustion mechanisms (e.g., strength and size of the recirculation zone, volumetric heat release patterns, liquid fuel evaporation and consumption characteristics, etc.) are inextricably linked to the jet mixing processes (see Figure 1). Clearly, advances in gas turbine combustor technology are dependent upon and cannot occur without understanding jet mixing into confined cross flows.

---

† Associate Director, UCICL, Member AIAA
‡ Student, Member AIAA
§ Professor, Associate Fellow AIAA
†† Senior Researh Engineer, Assoc. Fellow AIAA

The need to understand and optimize jet mixing into cross-flows is not limited to gas turbine combustor applications. Similar mixing problems exist in the design of fuel and air premixers, the discharge of effluent into water, and many other applications where two continuously flowing streams are mixed together.

The present study addresses the fundamental mixing characteristics that govern the optimal mixing in cylindrical ducts. The goals of the present study are to (1) characterize the relationship between the jet orifice geometry and number as it relates to mixture uniformity one duct radius downstream of the orifice leading edge for a fixed jet-to-mainstream momentum-flux ratio, and (2) identify the optimal mixing configuration.

Background

Many recent studies have been conducted relative to jet mixing in gas turbine combustor applications. These studies have been focused on both cylindrical[1-8] and rectangular[9-17] duct configurations. In these studies, the importance of the momentum-flux ratio, orifice shape and orifice number are delineated.

Hatch et al.[1] studied the mixing characteristics of both circular and slanted slot jet orifices in a cylindrical duct, where the number of orifices for each mixer was held constant at eight. Mixing quality was quantified at an axial distance equal to one duct radius downstream of the leading edge of the orifice using an area weighted standard deviation value for experimentally determined mixture fractions. The best mixer had the smallest value of area weighted standard deviation at the evaluation plane. Among other results, it was observed that the optimum mixing configuration likely varied in number of orifices at a fixed momentum-flux ratio. Consequently, because the number of orifices were not varied, an optimum mixer could not be identified.

In a study limited to round hole orifices, Kroll et al.[4] determined experimentally the optimum number of orifices for two fixed momentum-flux ratios of J=25 and J=52. The optimum number of round hole orifices for these momentum-flux ratios based on the same criteria as the Hatch et al.[1] study was found to be 10 and 15 respectively. (Further analysis determined that the actual experimental momentum-flux ratios were 36 and 70 for the J=25 and J=52 cases respectively.) The corrected results agreed well with the design equation reported by Holdeman[10,11]:

$$n = \pi\sqrt{2J} / C \qquad (1)$$

With C=2.5 (as suggested in(10)), the needed number of round hole orifices predicted by Equation (1) is 10 and 15 for the low and high momentum-flux cases reported in Kroll et al.[4] respectively.

Oechsle et al.[3] considered the optimization requirements of the different orifice designs reported in Hatch et al.[1]. They used several different parameters for optimization including the area weighted standard deviation discussed above. They concluded in part from their numerical and analytical study that relatively shallow-angled slanted slot orifices would provide optimum jet penetration and mixing characteristics.

Although the preceding studies have provided much insight on orifice optimization to achieve best mixing conditions in cylindrical ducts, none of the studies followed an optimization approach that systematically varied orifice design parameters at a fixed momentum-flux ratio such that a mathematical response surface could be created. This is the goal of the current study: to identify the sensitivity of jet mixing performance to small changes in orifice slot angle, aspect ratio, and orifice number. In the current study, odd shaped orifices are not considered.

Experiment

Facility. The experimental facility that was used for this research is the same basic test stand and flow panel that is described in Hatch et al.[1] and Kroll et al.[4]. This facility provided 212^{o}F main stream air at atmospheric pressure. Jet air was supplied at 74^{o}F to a manifold which supplied the orifices in the mixer. A thermocouple probe was used to measure the local temperature where the jet fluid mixed with the heated mainstream fluid.

Figure 2 depicts the arrangement of the test assembly and the thermocouple probe. The displacement of the three axes was monitored with a Mitutoya digital displacement indicator with a precision of 0.001 inch. The 1/8 inch type K thermocouple used for thermal flow field mapping was centered and aligned prior to each experiment.

The main (core) air flow enters the bottom of the mixing module at a temperature of 212 °F and a bulk velocity of 31 ft/sec. The manifold was manufactured with four ports equally spaced around the manifold's circumference at both the top and bottom. Four individually metered air streams supply the lower four manifold ports with jet air at approximately 74 °F. After entering the bottom of the manifold, the jet air flows upward through a 1/2 inch thick honeycomb ring. The honeycomb aids in removing any swirl from the jet air prior to its passage through the mixer's orifices.

One of the manifold's top ports is used to monitor the air pressure, a thermocouple is located in a second port to measure the jet temperature, and the remaining two ports are capped off. A dimensioned mixer is shown in Figure 3 for reference.

Probe Design. A thermocouple probe was chosen to perform the point temperature measurements in accordance with the desire to use a simple and reliable measurement technique. The relatively large time constant of the thermocouple had the effect of averaging the temperature fluctuations in the fully turbulent flow field. Four probe designs were investigated to evaluate which design minimized the flow field perturbations. Each probe design used a 12 inch long 1/8 inch diameter type-K thermocouple. The following criteria were established to evaluate alternative probe designs:

- The calculated jet fluid back-flow should be minimized and approach zero at the orifice leading edge.
- 100% of the jet fluid mass should be accounted for at the orifice trailing edge plane (z/h = 1.0).
- Deviation of the mean mixture fraction from the calculated equilibrium value at z/R=1.0 should be minimized.

The initial probe design was a straight, axially-aligned probe. Because this probe was aligned with the bulk fluid flow direction, it would perturb the flow the least downstream of the orifices. The experiments bore this out. For the straight axial-aligned probe, flow field perturbations were not significant except in the orifice region. However, in the vicinity of the orifices, the strong degree of cross-flow normal to the probe caused perturbations that resulted in the appearance of a high degree of jet fluid back-flow; (i.e., the propagation of jet fluid in the upstream direction).

To minimize the perturbations in the orifice region, three other thermocouple probe designs were analyzed. The first was an axially aligned probe with a 90 degree bend near the thermocouple junction. In this arrangement, the 90 degree section of the probe pointed into the oncoming jet stream, thereby eliminating the strong cross-flow that was problematic for the straight probe. Analysis of a data set collected with the 90 degree probe revealed that this arrangement was biased to the main stream flow. At the axial plane corresponding to the trailing edge of the orifices, the integrated 90 degree probe data did not show adequate mass balance closure. At the trailing edge plane well less than 100 percent of the jet mass was measured which result is not physically realistic. Where the straight probe was unrealistically cold in the orifice region (biased to the jets), the 90 degree probe was unrealistically hot (biased to the main stream). In both cases, the cross-stream fluid tended to bias the measurement.

On the basis of these results, an axially aligned probe with a 45 degree bend was selected and a third data set was collected for the same module (12 orifice round hole design at a jet to mainstream momentum-flux ratio of 36). Not surprisingly the 45 degree probe results fell almost exactly between the two extremes. Mass balance closure testing of the 45 degree probe data set showed that 100 percent jet mass addition was accounted for at the orifice trailing edge and not significantly upstream of the trailing edge. The differences between a shielded and a nonsheilded thermocouple probe were also investigated. No differences were observed. Consequently, an exposed junction, 45 degree thermocouple probe was used to acquire the entire data set reported herein.

Each of the orifice optimization experiments involved the measurement of eight planes of data. Six of the eight planes were concentrated in the orifice region where the strongest thermal gradients were located. Only eight planes of data were acquired due to tradeoff between having enough mixing detail while keeping the time associated with each experiment to a reasonable length. These eight planes were located as follows:

Plane 1:	z	=	-0.100	inches
Plane 2:	z	=	0.000	inches
Plane 3:	z	=	0.100	inches
Plane 4:	z	=	h/2	inches
Plane 5:	z	=	h-0.100	inches
Plane 6:	z	=	h	inches
Plane 7:	z	=	h+(R-h)/2	inches
Plane 8:	z	=	R	inches

where z=axial distance relative to the leading edge of the orifice, h=the orifice axial distance and R=mixer radius (1.5 inches). This paper focuses soley on results from Plane 8.

In each data plane (identified above), the data taking region comprised a two orifice sector. If the 2 orifice sector was less than (greater than) 90 degrees, then the grid was spatially compressed (expanded) so the relative density of the measurements was preserved. The gridding scheme followed in this study for a 90 degree two orifice sector is shown in Figure 4. The central portion of the grid is composed of a Cartesian type of scheme employing equal x,y increments. Additionally, data points are arranged in an equal increment fashion along the initial and final sector radial lines, as well as around the circumference of the sector.

Global Orifice Optimization. On the basis of the results reported in Hatch et al.[1] and Kroll et al.[4], a Box-Behnken test matrix was established for this study. The previous studies were used to identify parameter ranges that would encompass the optimal mixing geometry at a momentum-flux ratio of 40 and at a fixed jet-to-main stream mass flow ratio of 2.5. Table 1 shows the initial 13 cases (cases 1-13 respectively) and variable settings for each case. Three parameters were varied: number of orifices, slot aspect ratio and slot angle. As noted above, Figure 3 details the mixer design used. In this study all of the orifices had circular ends. Consequently, a slot with an aspect ratio of 1 corresponded to a round hole. The first 13 experiments tabulated in Table 1 are shown pictorially in Figure 5. The Box-Behnken test matrix allowed the fitting of non-linear regression equations to the data while minimizing the number of required experiments. The operating conditions are listed in Table 2.

Upon completion of the data acquisition for the initial 13 cases of Table 1, the mixture fraction standard deviation (STD) was calculated at each plane in the flow field to quantify the degree of mixedness at each plane. The z/R=1 axial plane for the initial 13 cases listed in Table 1 were repeated once to provide an estimate of pure experimental error. A regression analysis was performed on the results at the z/R=1.0 plane to arrive at a model that quantifies the STD as a function of the number of orifices, the orifice aspect ratio, and the orifice angle. The results of this regression analysis highlighted the need to conduct a second Box Behnken test matrix to better refine the response surface.

Cases 14-26 in Table 1 detail the second test matrix. This test matrix was identical to the first except that the number of orifices ranged between 6 and 10. When the measurements corresponding to cases 14-26 were completed, a cubic model was fit to the data sets and used to further understand the relationship between design parameters. Insignificant model terms were removed from the cubic equation using traditional statistical methods.

Analysis

The mixture fraction value is a measure of the degree of local mixedness or unmixedness at a given point. Temperature measurements were made as a means of tracking the local mixture fraction. This was possible, because the experiments were non-reacting. In this system, temperature is a conserved scalar (i.e. no sources or sinks). Conserved scalars can track other conserved scalars (e.g. local elemental mass fractions) in a non-reacting system[18].

The mixture fraction takes the following form when based on temperatures:

$$f = \frac{T_{local} - T_{jet}}{T_{main} - T_{jet}} \qquad (2)$$

A value of f=1.0 corresponds to the presence of pure main-stream flow, while f=0 indicates the presence of pure jet flow. Note that this definition is opposite to some previous definitions in the literature (e.g., ref (10)). Complete mixing occurs when f approaches the equilibrium value determined by the mass-flow ratio and temperatures of the jet and main-stream.

To quantify the mixing effectiveness of each mixer configuration, an area-weighted standard deviation parameter ("STD") was defined at each measurement and interpolated data plane.

$$STD = \sqrt{\frac{1}{A}\sum a_i (f_i - \bar{f})^2} \qquad (3)$$

where f_i is the average planar mixture fraction. a_i is the nodal area at which f_i is calculated, and A= Σa_i. It should be noted that at planes downstream of the trailing edge of the orifice, $\bar{f}$ equals the equilibrium mixture fraction. Complete mixing is achieved when the STD across a given plane reaches zero.

Results

Table 1 lists the orifice axial distance and the percentage of orifice blockage for the 26 configurations considered. The orifice axial distance is expressed as the ratio of the axial projection of the orifice (h) to the radius of the mixing module (R=1.5 inches). The percent blockage is expressed as a ratio of the total circumferential projection of the orifices to the circumference of the mixer.

The normalized orifice axial distance (h/R) is a measure of the axial rate of jet mass addition. To illustrate its importance to mixing, consider two extreme cases; h/R=1.0 and h/R≈0.0. For the case where h/R=1.0, the jet fluid addition process is continuing right up to the final mixing analysis plane at z/R=1.0. The jet fluid that passes through the trailing portion of the orifice does not have the opportunity to mix with the main fluid. This results in warm and cool spots in the analysis plane and a correspondingly high mixture fraction standard deviation. At the other extreme is the case where h/R ≈0.0. This corresponds to the jet fluid being added instantaneously, thereby having the entire residence time between z/R=0.0 and z/R=1.0 to mix with the main fluid. Note that in the six orifice case (number=6, aspect ratio=5, angle=30, see Table 3), the orifice axial distance extends beyond one duct radius downstream. Also in a few of the other six and eight orifice cases, the orifice axial distance is nearly equal to one duct radius.

The percentage of orifice blockage for a given orifice long-to-short aspect ratio and number of orifices is inversely proportional to the orifice axial distance. A high aspect ratio design at a zero degree orifice inclination angle (aligned with the mixer's center-line) would have a large h/R and a small percentage of orifice blockage. The opposite is also true.

As the percentage of orifice blockage approaches 100, the jet flow approaches the point of completely inhibiting the flow of the main fluid near the module's wall. This can have the advantage of cooling the walls at the expense of allowing an undiluted core of main fluid to pass through the mixer section. Similarly, with an orifice angle of zero (i.e., no orifice induced swirl component), as the percentage of orifice blockage approaches zero, the jet penetration would be great and a large portion of the walls would be exposed to undiluted main fluid while the jets impinged upon one-another at the module's centerline. Slotted orifice designs at non-zero orifice angles act as swirl vanes to the approaching main-flow. In the consideration of jet penetration, the swirl component imparted on the main-flow must be considered.

The round hole cases had blockage values that were less than slots at angles exceeding 34 degrees at an aspect ratio of 1.5 and 22 degrees at an aspect ratio of 5.0. Note that all orifices at angles greater than 40 degrees (AR > 1.001) have a blockage greater than round hole orifices. The orifice blockage in and of itself was not solely responsible for the degree of mixedness at one duct radius downstream.

Mixture Fraction Contours at z/R=1.0. Figure 6 shows diagramatically the orifice aspect ratio and angles experimentally evaluated for the 16 orifice case. The mixture fraction contour plots at one duct radius downstream of the orifice leading edge (z/R=1.0) are shown in Figure 7 for the 16 orifice case. Each case in Figure 7 represents a two orifice measurement sector that has been orifice averaged. Similar figures for the 12, 10, 8 and 6 orifice cases are shown in Figures 8-14 respectively. The variable levels depicted in Figures 6, 8, 10, 12, and 14 can be compared one-to-one to their corresponding contour plots in Figures 7, 9, 11, 13, and 15 by noting the relative position of an image in the later figures with the corresponding test matrix point in the test matrix diagrams. In each of the mixture fraction contour plots, each contour image is labeled with a numerical designator of the form: number/aspect ratio/angle. For example, 16/3/30 signifies the 16 orifice module at a long-to-short aspect ratio of 3 and an orifice angle of 30 degrees from the module's centerline. In the contour plots, a mixture fraction value of 1 corresponds to pure main flow material, a value of 0 corresponds to pure jet flow material. Because an aspect ratio of one corresponds to a round hole, the performance of an aspect ratio=1 mixer is independent of orientation angle. In the figures that follow, for convenience, the aspect ratio equal to one cases are associated with an angle corresponding to what the Box-Behnken test matrix would call for if the angle could be uniquely specified at that condition.

All four of the sixteen orifice cases shown in Figure 7 demonstrate under-penetrating jets. This is evident by the high mixture fraction values on the mixer centerline. (If the jet penetration were balanced, a band of mixture fraction values containing the equilibrium value (.285) would be present with a band of slightly higher mixture fraction values near the mixer centerline and wall.) Table 3 lists the computed area weighted standard deviations about the mean mixture fraction values for all of the cases depicted in Figures 7-15. For the sixteen orifice case, the best value of area weighted standard deviation (closest to zero) is the 16/3/0 case which is a slot aligned with the main flow. This is due to the fact that it has no induced swirl motion as do cases 16/3/60 and 16/5/30, and has much less blockage than the 16/1/30 case.

As was seen with sixteen orifices, the twelve orifice cases are largely under-penetrating (see Figure 9). However, the mixing is in some cases much improved over the sixteen orifice cases. The 12/5/0 case is the most balanced case and has the lowest area weighted standard deviation (0.068). This, as was true for 16/3/0, results from a low blockage and no induced swirl because it is aligned with the main flow. The good mixing performance at one duct radius downstream is especially interesting given the fact that the axial orifice distance extends close to the evaluation plane (see Table 3).

Of all of the cases considered the 10 orifice modules displayed the best mixing performance based on the area weighted standard deviations (see Table 3). In Figure 11, only the 10/3/60 case displays significant under-penetration. This under-penetration is highly correlated with the swirl induced by the steep orifice angle. The sensitivity of mixing performance to blockage is less important as the number of orifices approaches the optimum number. In the better mixed cases, only two color ranges are represented that are close to the equilibrium mixture fraction value (0.285). As was discussed in Kroll et al.[4], it can be seen that the optimum mean jet penetration depth falls between the half area radius and the linear half radius in the mixer as determined by the radial location where the lowest mixture fraction is measured in the evaluation plane.

The eight orifice module cases were the overlap condition between the two Box-Behnken test matrices discussed above. The seven cases are shown in Figure 13. Recall that the aspect ratio equal one case is angle-independent. In the eight orifice cases, jet under-, balanced- and over-penetration is evident. The steep orifice angles still exhibit under-penetration likely due to the strong induced swirl. The no swirl cases, 8/5/0, 8/3/0, and 8/1/angle-independent show a tendency towards over-penetration. For eight orifices, however, the greater blockage of the 8/1/angle-independent case improves the mixing. The 8/5/30, 8/3/30, and 8/1/angle-independent all showed excellent mixing performance that is equivalent to the ten orifice good mixing cases especially when considering the degree of case-to-case repeatability.

In Figure 15, the six orifice cases are shown. With six orifices, only the steep-angled slanted slot orifice case 6/3/60 shows balanced jet penetration. The area weighted standard deviation for this case (0.051) is close to the best values measured in the eight and ten orifice cases. All of the other six orifice cases are over-penetrating and consequently display degraded mixing performance. In some cases the orifice heights extend up to (6/3/0) and beyond (6/5/30) the evaluation plane.

Figure 16 shows four repeat measurement for the 8 round hole orifice case (not orifice averaged). The repeat cases are representative of the repeatability seen in all of the experiments. The values of area weighted standard deviation for the repeat cases shown in Figure 16 are 0.0536, 0.0585, 0.0438 and 0.0599. In general the measured repeatability in the area weighted standard deviation was on the order of 0.015. The cases that had the steepest gradients in the measured mixture fraction generally had the worst repeatability in the area weighted standard deviation.

Linear Regression Analysis. In order to further generalize the results, a linear regression was performed on 63 values of area weighted standard deviation generated from the 26 cases noted above using the Rummage II (see ref. (19)) statistical analysis software. An interpolating equation was created for the area weighted standard deviation (STD) as a function of the three experimental parameters; i.e., the number of orifices (n), the orifice aspect ratio (AR), and the orifice angle (α). Insignificant terms were eliminated from the model using conventional statistical methods. The regression model took into account the fact that at an aspect ratio of 1, the resulting STD had to be angle-independent. The regression data was scaled to remove any unnecessary ill-conditioning due to the data ranges considered. The resulting equation is:

$$STD = C_0 + C_1*x_1 + C_2*x_2 + C_3*x_3 + C_4*x_1*x_1 + C_5*x_3*x_3 + C_6*x_1*x_2 + C_7*x_1*x_3 + C_8*x_2*x_3 + C_9*x_1*x_1*x_1 + C_{10}*x_1*x_1*x_3 \quad (4)$$

where: x_1 = (n-10.28571)/3.36696
x_2 = (AR-2.23810)/1.58332
x_3 = ((α*(AR-1))-37.14286)/65.92832

C_0 =	0.059439	C_1 =	0.026584
C_2 =	-0.004550	C_3 =	0.011859
C_4 =	0.027561	C_5 =	0.010224
C_6 =	-0.013867	C_7 =	0.018288
C_8 =	-0.009102	C_9 =	-0.009068
C_{10} =	-0.008064		

The regression equation had a correlation coefficient of 0.926, and an estimated standard deviation of 0.011. Although potential outliers were identified in the data set, no data was removed when fitting the regression equation. Not removing the outliers resulted in six of the 63 data points accounting for 46.6 percent of the regression sum of squares error.

Figure 17 shows the predicted values of STD as number of orifices, orifice aspect ratio and orifice angle are changed. Many of the observations made in the previous figures can be more easily seen. For example, only in the six orifice case is the steep-angled slot at a high aspect ratio an advantage. As the number of orifices increases, the steep-angled slot at a high aspect becomes poorer and poorer. At high orifice numbers, a zero angled slot at a high aspect is the best. Second, the highly nonlinear relationship between the three controlled variables is evident. It was this highly nonlinear relationship that required introducing third order cross terms into the correlation equation. Third, it is evident that the optimum number of orifices falls between nine and ten orifices when the area weighted standard deviation is the optimizing parameter. Fourth, it is also evident that in the near optimum configuration, the orifice aspect ratio is of lesser importance as long as the orifice angle is shallow.

The independence of orifice aspect ratio when using shallow-angled orifices at the optimum number of orifices is better understood by considering a contour plot for the 9 orifice case shown in Figure 18. In this figure, two optimums are present. One optimum is at an aspect ratio of 1 and the second optimum is at an aspect ratio of 5 and an orifice angle of 20. Given the uncertainty in the measurements (discussed above), one could expect equally good mixing performance at many combinations of shallow-angled slanted slots, and aspect ratios. The existence of two optimums is also predicted in the 8 and 10 orifice cases. When the orifice number increases beyond 10, only one optimum is predicted at high aspect ratios and shallow angles.

In an effort to verify the existence of two optimums, two additional cases were considered: 9/1/angle-independent and 9/5/22. The contour plots for these cases are shown in Figure 19. The 9/1/angle-independent case demonstrated an experimentally derived area weighted standard deviation of 0.052, which is close to the predicted value of 0.050. The 9/5/22 case displayed greater jet penetration to the centerline than expected. This resulted in an experimentally derived area weighted standard deviation of 0.065 which is higher than the predicted value of 0.052. Because the repeatability of the measurement of STD (as discussed above) is on the order of 0.015, the 9/5/22 STD result is within the uncertainty band. However, this experimental result for the 9/5/22 case is somewhat anomolous since the 10/5/30 and the 8/5/30 cases (see Figures 11 and 13) both display balanced jet penetration. It is, however, possible that the nonlinear sensitivity of the interpolating equation is not sufficient. Consider, for example, that the 8/5/0 case does display jet overpenetration.

Summary and Conclusions

This study focused on understanding the relationship between number of orifices, orifice aspect ratio and orifice angle at a fixed momentum-flux ratio (40) in a plenum fed cylindrical can mixer. The mixture fraction field at one duct radius downstream of the leading edge of the orifices was measured experimentally using thermocouples in a non-reacting flow field. The mixture fraction fields as well as the

area weighted standard deviations were used to assess mixing performance. A general interpolating equation was found using least-squares regression that was used to further elucidate the trends. The orifice optimization experiments resulted in the following conclusions:

1. Mixture uniformity is a non-linear function of the number of orifices, the orifice long-to-short aspect ratio, and the orifice angle.
2. Jet penetration depth appears to be a function of circumferential blockage, axial jet mass addition rate, and orifice induced swirl.
3. Optimum mixing occurs when the asymptotic mean jet trajectories are in the range of $0.35 < r/R < 0.5$ (where r=0 is at the mixer wall) at $z/R = 1.0$.
4. An optimum number of orifices does exist for a given momentum-flux ratio which minimizes the mixture uniformity value. Although there is an overall minimum for a given momentum-flux ratio, there is also a local minimum for a given number of orifices. Thus the appropriate configuration may depend on given values of both the momentum-flux ratio and the number of orifices.
5. When the optimum number orifices are exceeded, steep-angled slanted slots lead to extremely poor mixing performance. In this case aligned slots that minimize the blockage without inducing swirl will provide the best mixing performance.
6. At the optimum number of orifices, the difference between shallow-angled slots with large aspect ratios and round holes is minimal and either approach will lead to good mixing performance. At the optimum number of orifices, it appears possible to have two local optimums where one corresponds to a round hole and the second to a shallow-angled slanted slot.
7. When the number of orifices are below the optimum number, there is an advantage to having steep-angled slanted slots at a high aspect ratio. In this case the slot induced swirl minimizes the degree of over-penetration.
8. Understanding how the number of slots, orifice aspect ratio and orifice angle relate to one another provides a means to further address design issues as load changes in devices that rely on jet mixing as an inherent part of their operation.

Acknowledgment

This work was made possible by support provided by NASA-Lewis Research Center (Grant NAG3-1110).

References

1. Hatch, M.S., Sowa, W.A., Samuelsen, G.S., and Holdeman, J.D., "Jet Mixing Into a Heated Cross Flow in a Cylindrical Duct: Influence of Geometry and Flow Variations," AIAA-92-0773, 1992. (also NASA TM 105390).
2. Oechsle, V.L., Mongia, H.C., and Holdeman, J. D., "A Parametric Numerical Study of Mixing in a Cylindrical Duct," AIAA-92-3088, 1992. (also NASA TM 105695).
3. Oechsle, V.L., Mongia, H.C., and Holdeman, J. D., "An Analytical Study of Jet Mixing in a Cylindrical Duct," AIAA-93-2043, 1993.
4. Kroll, J.T., Sowa, W.A., Samuelsen, G.S., and Holdeman, J.D., "Optimization of Circular Orifice Jets Mixing Into a Heated Cross Flow in a Cylindrical Duct," AIAA-93-0249, 1993 (also NASA TM 105984).
5. Talpallikar, M.V., Smith, C.E., Lai, M.C., and Holdeman, J.D., "CFD Analysis of Jet Mixing in Low NOx Flametube Combustors," J. Eng. Gas Turbine Pwr. **114**, 416 1992. (Also ASME Paper No. 91-GT-217; NASA TM 104466).
6. Vranos, A., Liscinsky, D.S., True, B., and Holdeman, J.D., "Experimental Study of Cross Stream Mixing in a Cylindrical Duct," AIAA Paper No. 91-2459, 1991. (Also NASA TM 105180).
7. Zhu, G., and Lai, M.-C., "A Parametric Study of Penetration and Mixing of Radial Jets in Necked-Down Cylindrical Cross-Flow," AIAA Paper No. 92-3091, 1992.
8. Howe, G.W., Li, Z., Shih, T.I.-P., and Nguyen, H.L., "Simulation of Mixing in the Quick Quench Region of A Rich Burn - Quick Quench Mix - Lean Burn Combustor," AIAA Paper No. 91-0410, 1991.
9. Doerr, Th., and Hennecke, D.K., "The Mixing Process in the Quenching Zone of the Rich-Lean Combustion Concept," AGARD-PEP 81st Symposium of Fuels and Combustion Technology for Advanced Aircraft Engines, 1993.

10. Holdeman, J.D., Srinivasan, R., Reynolds, R., and White, C.D. "Studies of the Effects of Curvature on Dilution Jet Mixing," J. of Propulsion and Power, Vol. 7, no. 4, Jul-Aug 1991.

11. Holdeman, J.D., "Mixing of Multiple Jets with a Confined Subsonic Crossflow," Prog. Energy Combust. Sci., **19**, pp. 31-70, 1993. (Also AIAA Paper No. 91-2458, 1991; and NASA TM 104412).

12. Smith, C.E., "Mixing Characteristics of Dilution Jets in Small Gas Turbine Combustors," AIAA-90-2728, 1990.

13. Smith, C.E., Talpallikar, M.V., and Holdeman, J.D. "Jet Mixing in Reduced Areas for Lower Combustor Emissions in Gas Turbine Combustors," AIAA 91-2460, 1991. (also NASA TM 104411).

14. Liscinsky, D.S., True, B., Vranos, A., and Holdeman, J. D., "Experimental Study of Cross-Stream Mixing in a Rectangular Duct," AIAA-92-3090, 1992. (also NASA TM 105694).

15. Bain, D.B., Smith, C.E., and Holdeman, J.D. "CFD Mixing Analysis of Jets Injected from Straight and Slanted Slots into Confined Crossflow in Rectangular Ducts," AIAA 92-3087, 1992. (also NASA TM 105699).

16. Bain, D.B., Smith, C.E., and holdeman, J.D., "CFD Mixing Analysis of Axially Opposed Rows of Jets Injected Into Confined Crossflow," AIAA Paper 93-2044, June 1993. (also NASA TM 106179).

17. Liscinsky, D.S., True, B , and Holdeman, J.D., "Experimental Investigation of Crossflow Jet Mixing in a Rectangular Duct," AIAA Paper 93-2037, June 1993. (also NASA TM 106152).

18. Smoot, L.D., and Smith, P.J., *Coal Combustion and Gasification*, Plenum Press, New York, 1985.

19. Bryce, G.R., "Data Analysis in RUMMAGE- A User's Guide," Department of Statistics, Brigham Young University, Provo, Utah, November 1982.

Table 1 Box-Behnken Test Parameters

Case	Number of Orifices	Orifice Aspect Ratio	Orifice Angle	h/R	Blockage[1] (%)
1	16	5	30	0.639	110
2	16	3	0	0.563	47
3	16	3	60	0.375	132
4	16	1	angle-independent	0.353	90
5	12	5	0	0.826	31
6	12	5	60	0.495	144
7	12	3	30	0.592	83
8,9	12	1	angle-independent	0.408	78
10	8	5	30	0.904	79
11	8	3	0	0.796	34
12	8	3	60	0.531	94
13	8	1	angle-independent	0.500	64
14	10	5	30	0.808	88
15	10	3	0	0.712	38
16	10	3	60	0.475	105
17	10	1	angle-independent	0.447	72
18	8	5	0	1.012	26
19	8	5	60	0.607	119
20	8	3	30	0.725	68
21,22	8	1	angle-independent	0.500	64
23	6	5	30	1.044	68
24	6	3	0	0.919	29
25	6	3	60	0.613	82
26	6	1	angle-independent	0.577	56

Table 2 Global Optimization Operating Conditions

T_{main} (°F)	T_{jet} (°F)	P (psia)	V_{main} (ft/s)	M_{main} (lbm/s)	Mass-flow Ratio	Density Ratio
212	74	14.7	31.0	0.090	2.5	1.28

[1]Blockage is defined as the sum of the circumferential length of each orifice divided by the circumference of the mixer.

Table 3 Area Weighted Mixture Fraction Standard Deviation

Number of Orifices	Orifice Aspect Ratio	Orifice Angle	Area Weighted Mixture Fraction Standard Deviation
16	5	30	0.125*
16	3	0	0.115*
16	3	60	0.165*
16	1	angle-independent	0.150*
12	5	0	0.068*
12	5	60	0.160*
12	3	30	0.075*
12	1	angle-independent	0.082*
10	5	30	0.044
10	3	0	0.046
10	3	60	0.105
10	1	angle-independent	0.050*
8	5	30	0.057*
8	3	0	0.076*
8	3	60	0.075*
8	1	angle-independent	0.054*
8	5	0	0.084
8	5	60	0.104
8	3	30	0.050
6	5	30	0.089
6	3	0	0.113
6	3	60	0.051
6	1	angle-independent	0.093*

*average of at least two repeat measurements

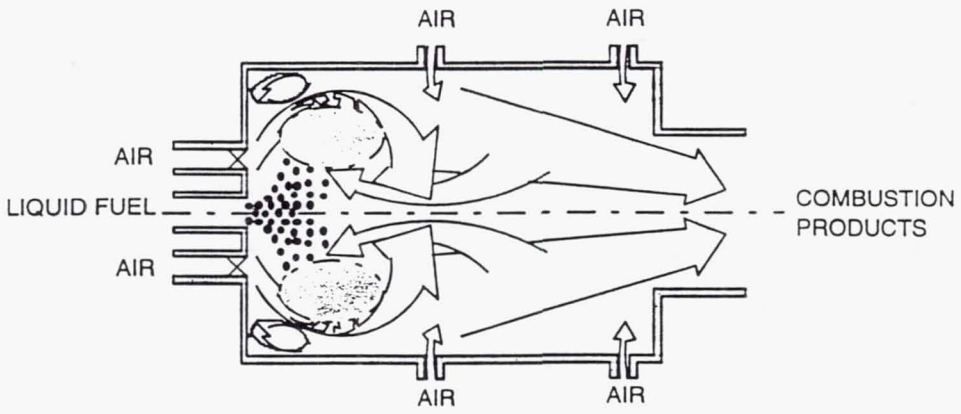

Figure 1. Schematic of a Gas Turbine Combustor.

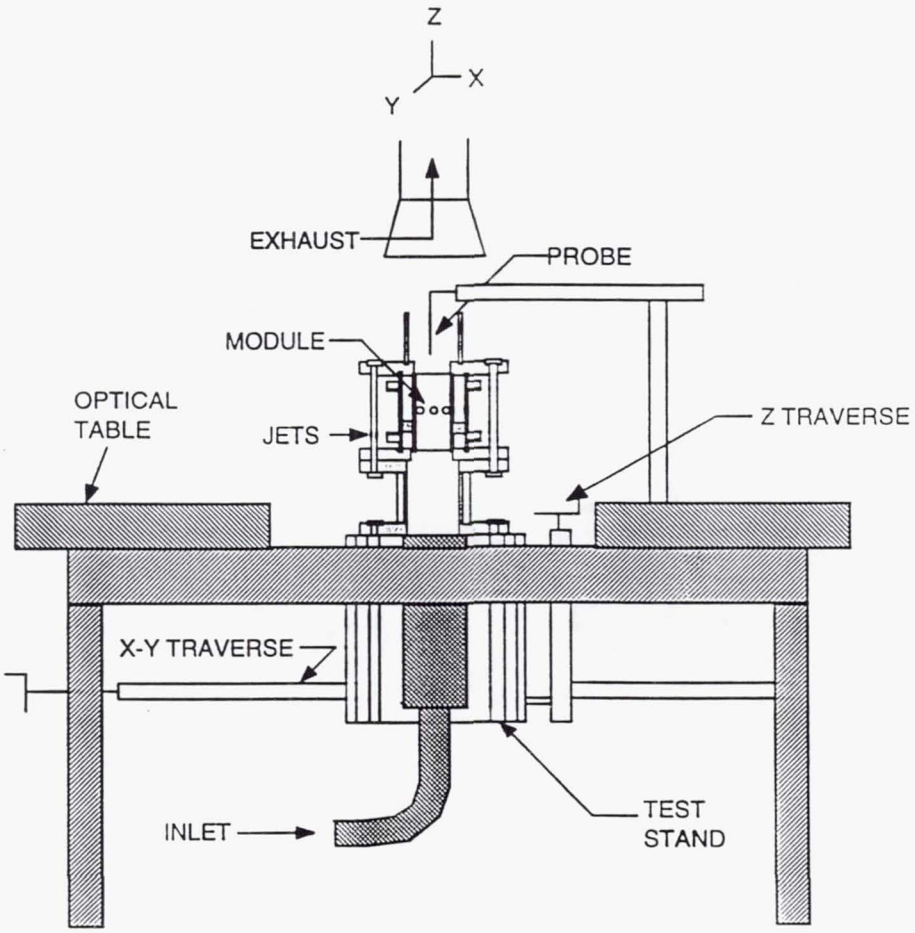

Figure 2. Test Stand Schematic

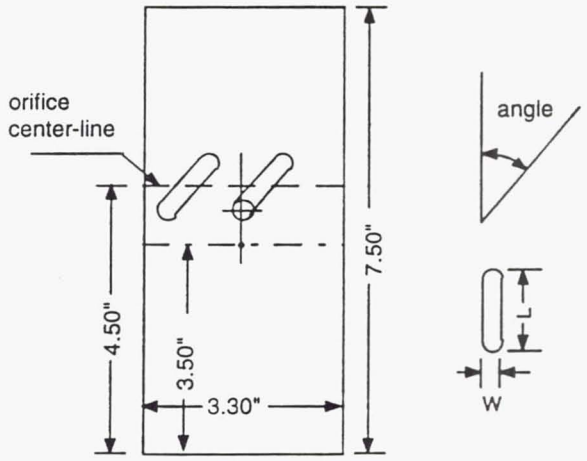

Figure 3. Mixing Module Dimensions

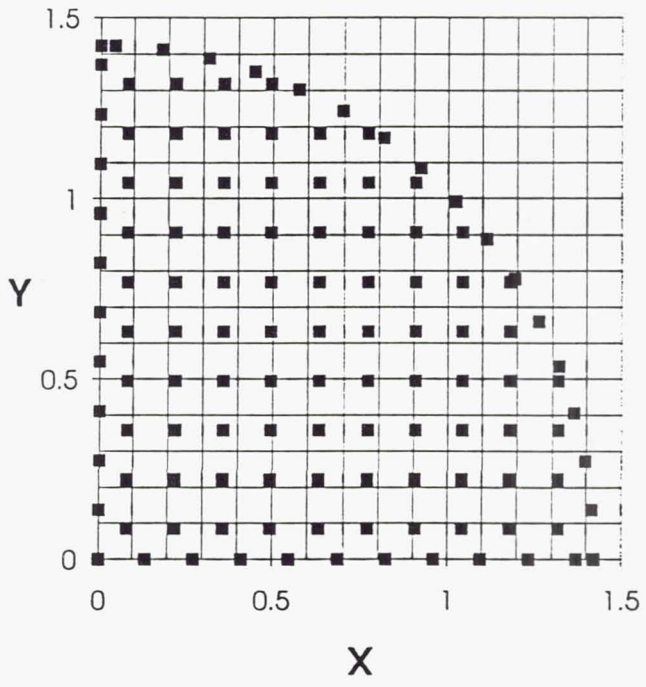

Figure 4. Example 90 Degree, Two Orifice Sector Planar Data Point Grid Density

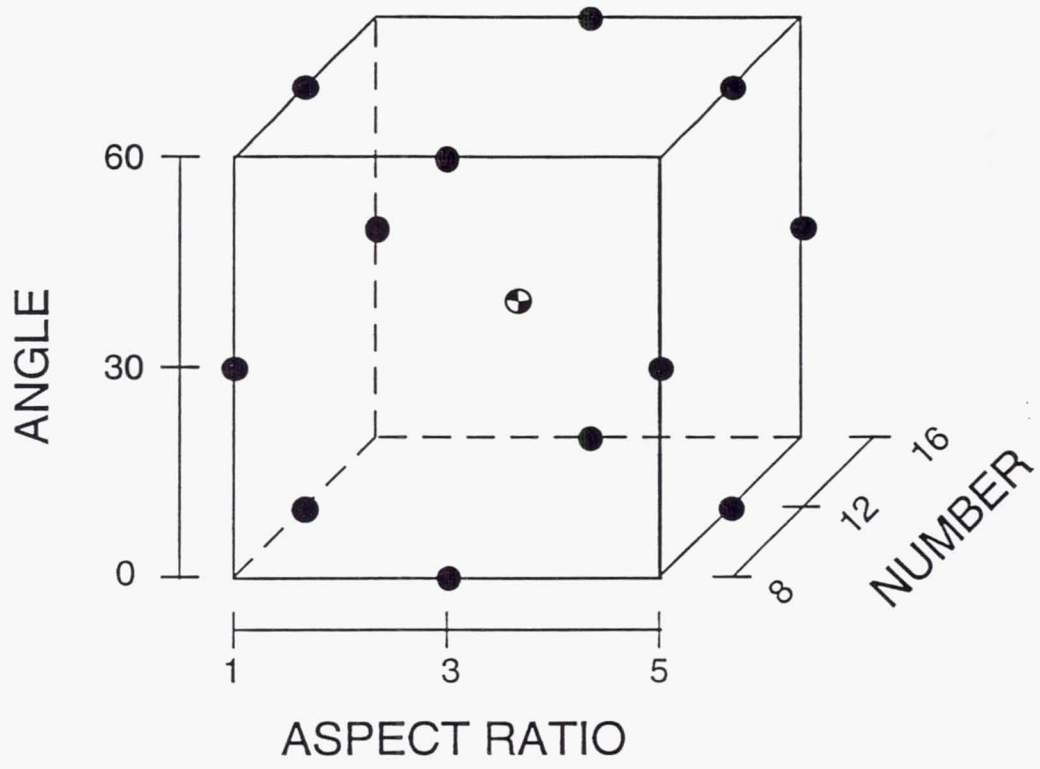

Figure 5. Graphical Illustration of Box-Behnken Test Matrix.

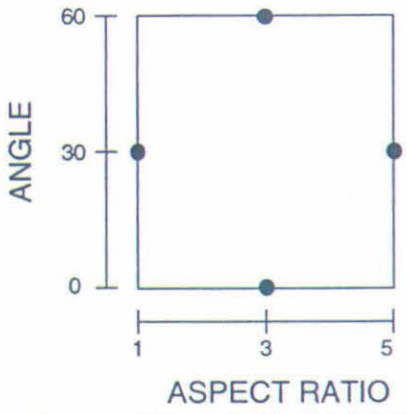

Figure 6. Sixteen Orifice Modules' Design Plane

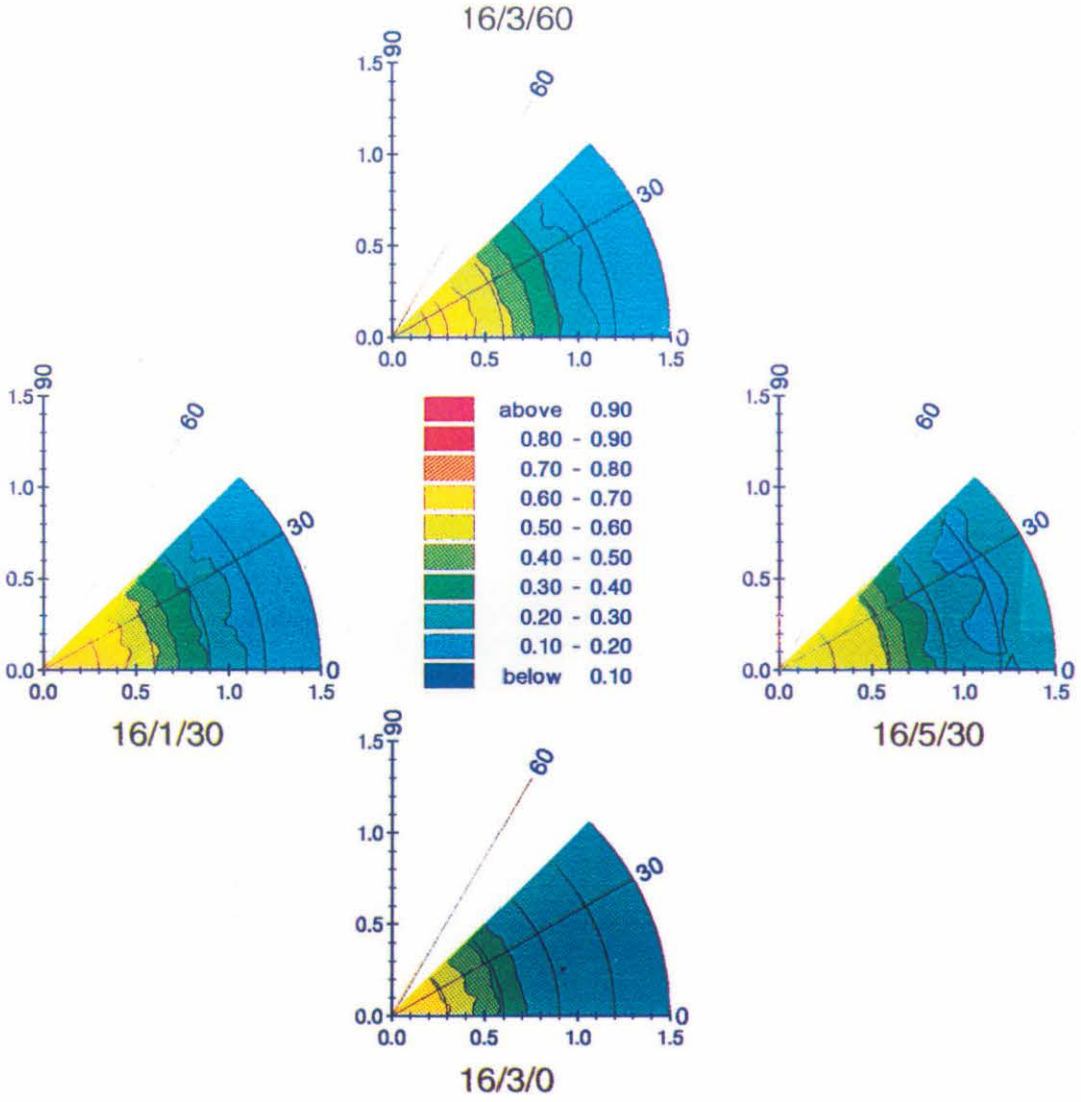

Figure 7. Sixteen Orifice Modules' Mixture Fraction Contours at z/R=1.0

Page intentionally left blank

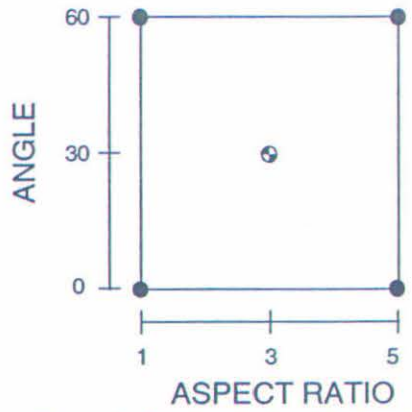

Figure 8. Twelve Orifice Modules' Design Plane

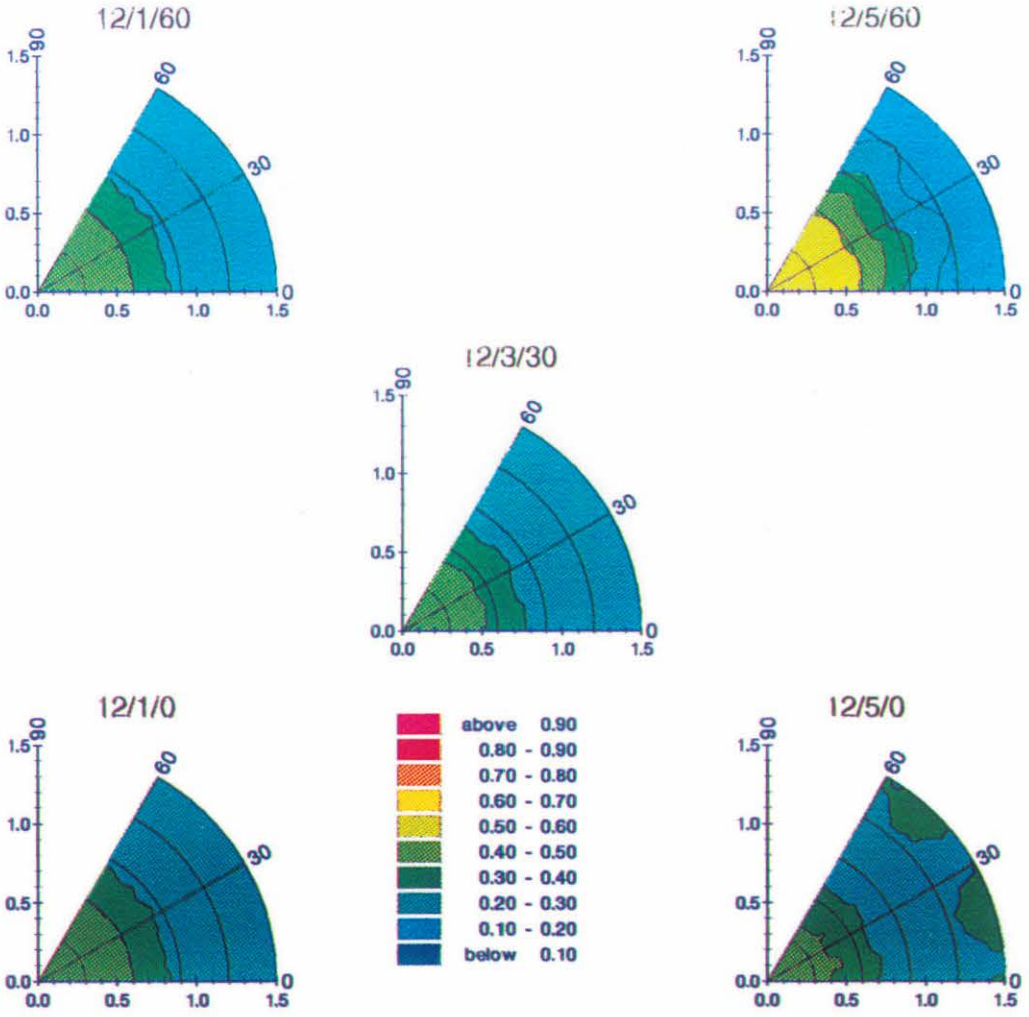

Figure 9. Twelve Orifice Modules' Mixture Fraction Contours at z/R=1.0

Page intentionally left blank

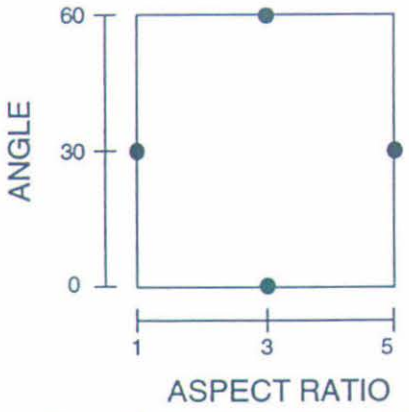

Figure 10. Ten Orifice Modules' Design Plane

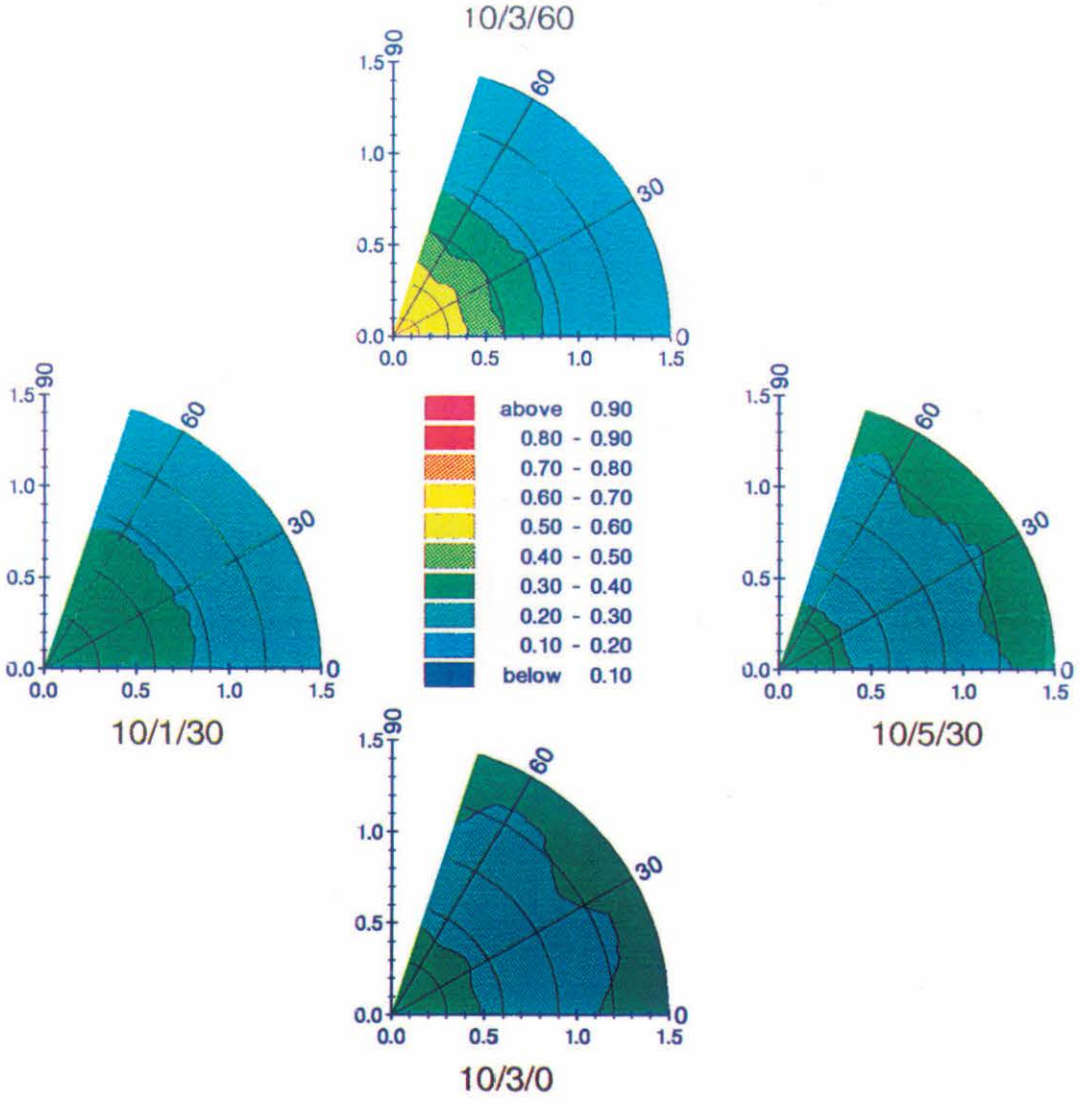

Figure 11. Ten Orifice Modules' Mixture Fraction Contours at z/R=1.0

Page intentionally left blank

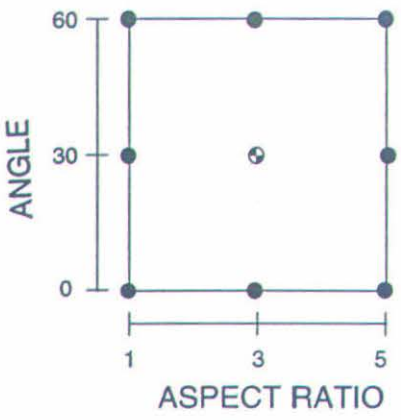

Figure 12. Eight Orifice Modules' Design Plane

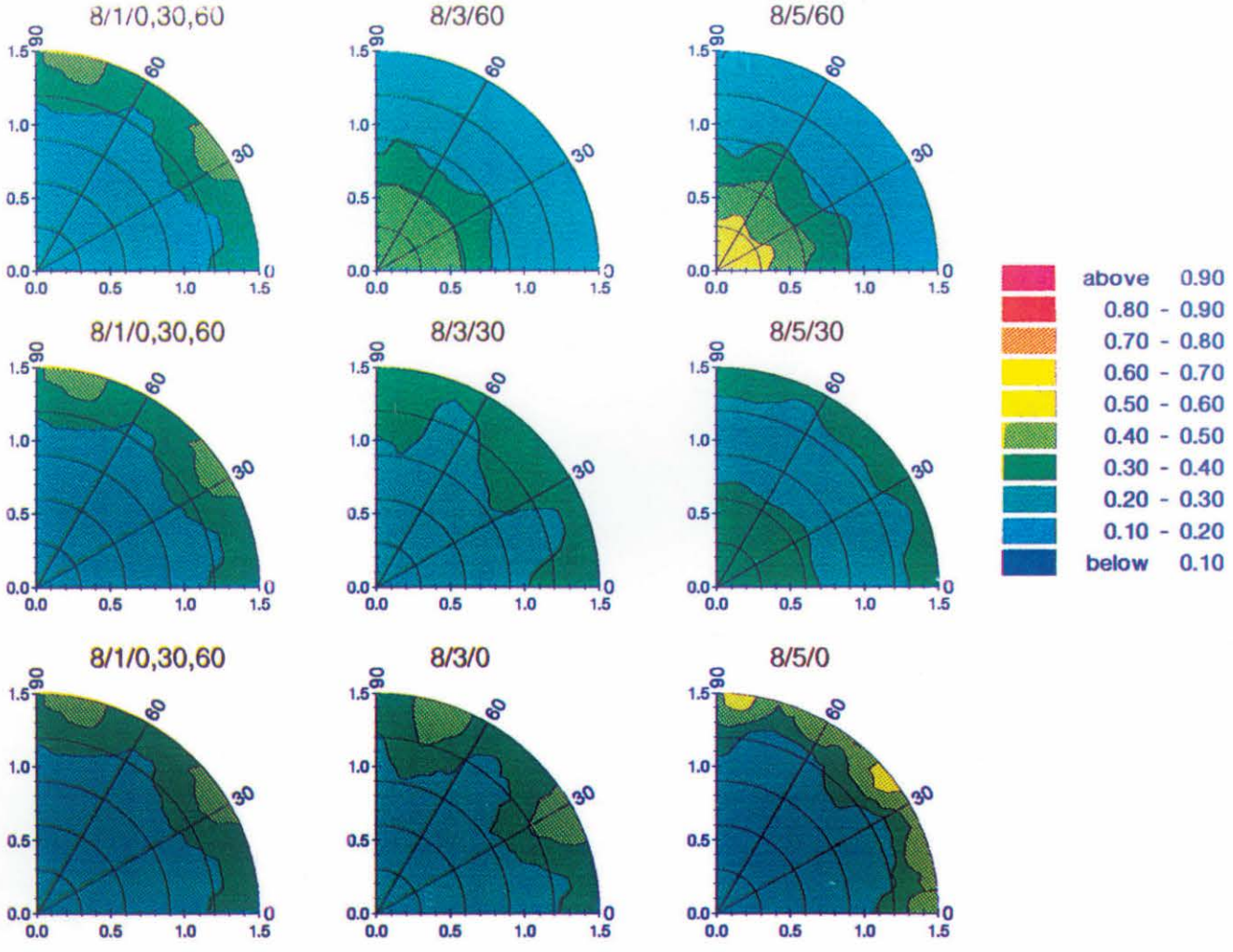

Figure 13. Eight Orifice Modules' Mixture Fraction Contours at z/R=1.0

Page intentionally left blank

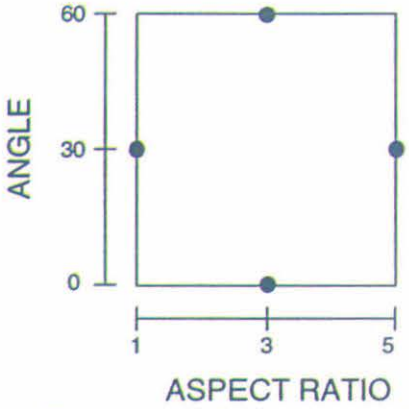

Figure 14. Six Orifice Modules' Design Plane

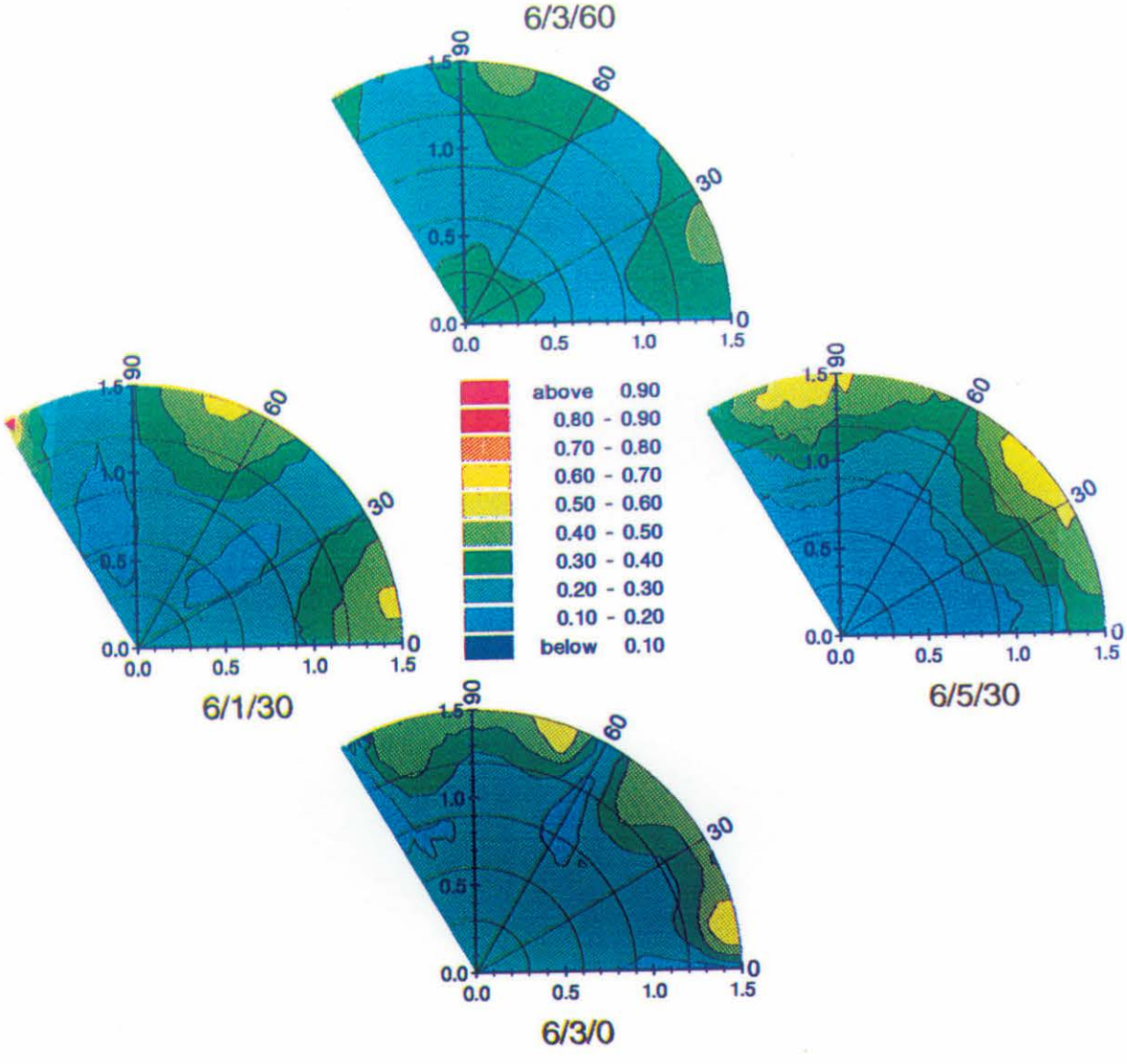

Figure 15. Six Orifice Modules' Mixture Fraction Contours at z/R=1.0

Page intentionally left blank

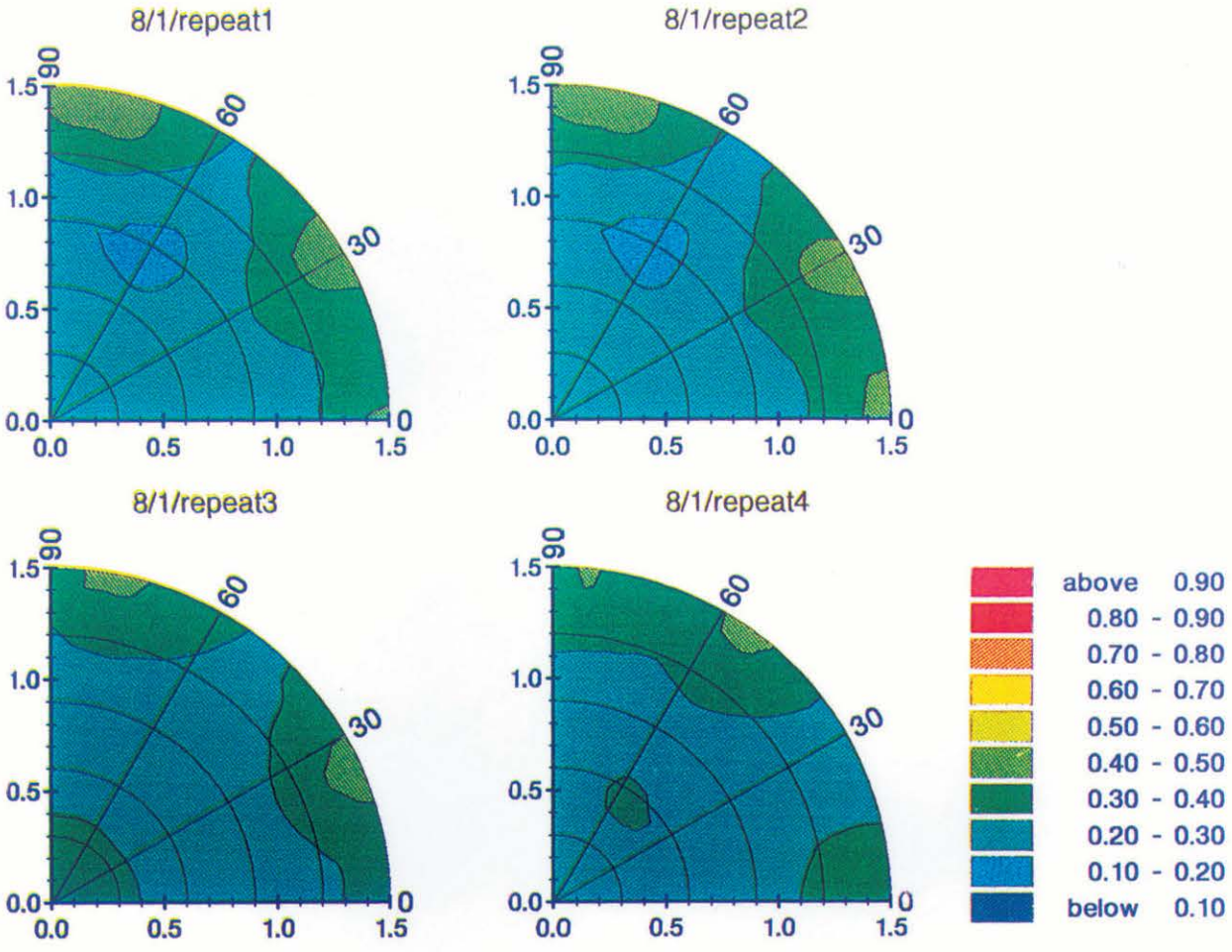

Figure 16. Repeatability of Planar Mixture Fraction Measurements for Three Repeat Cases of 8/1/angle-independent.

Page intentionally left blank

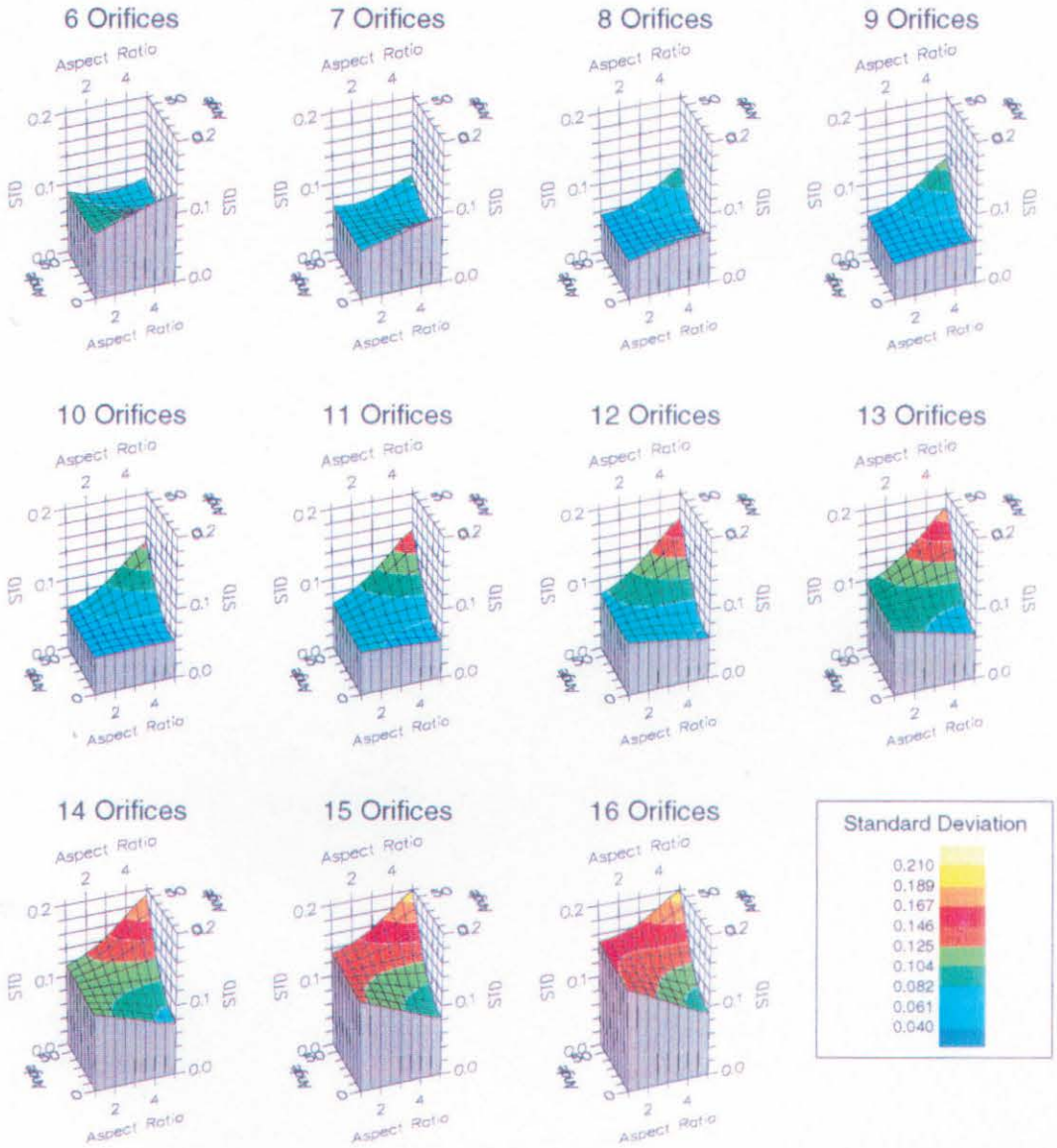

Figure 17. Predicted Values of Area Weighted Standard Deviation "STD" for Different Orifice Numbers as Orifice Aspect Ratio and Orifice Angle are Changed

Page intentionally left blank

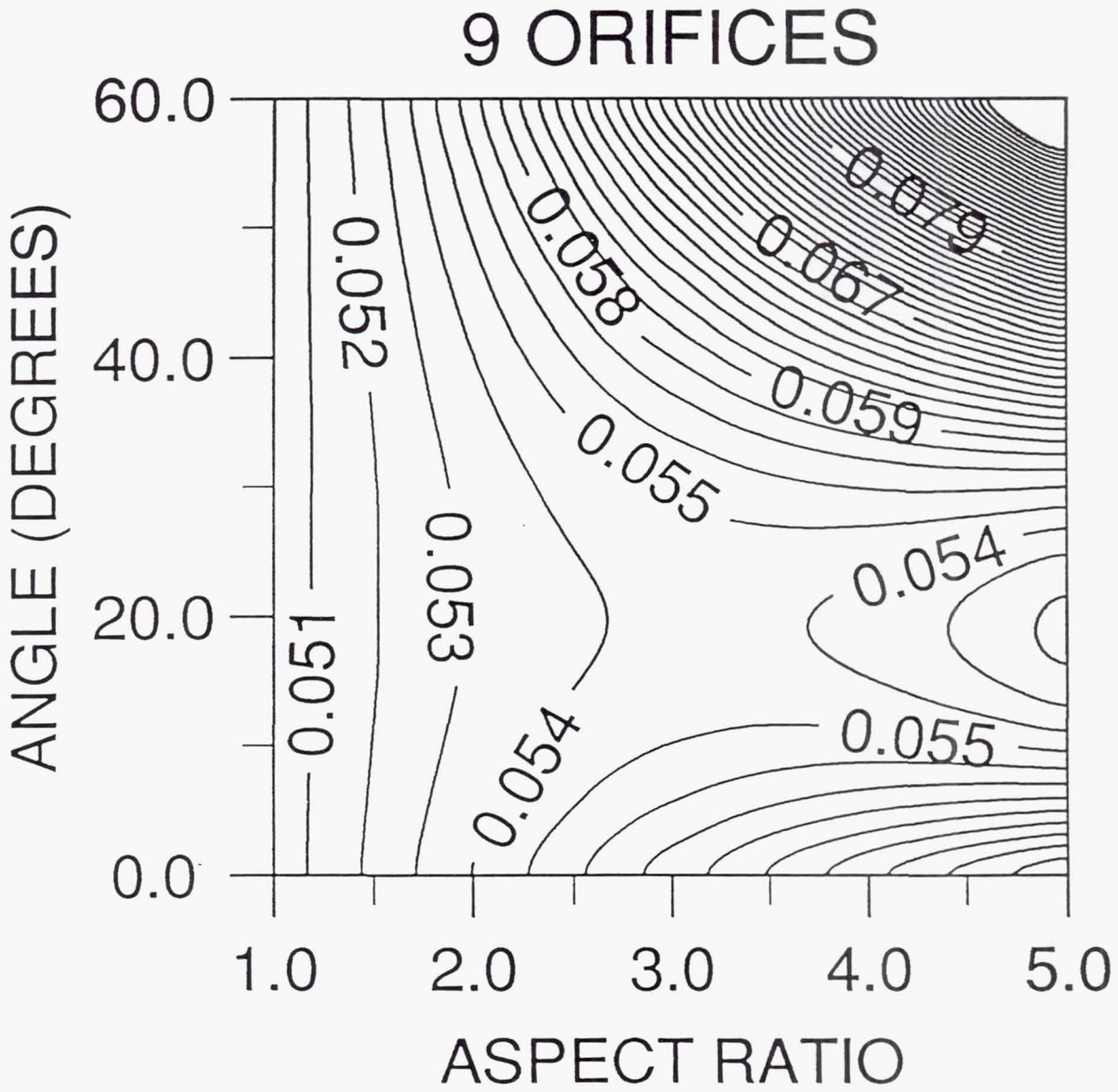

Figure 18. Predicted Values of Area Weighted Standard Deviation "STD" for the Nine Orifice Case as Orifice Aspect Ratio and Orifice Angle are Changed

Page intentionally left blank

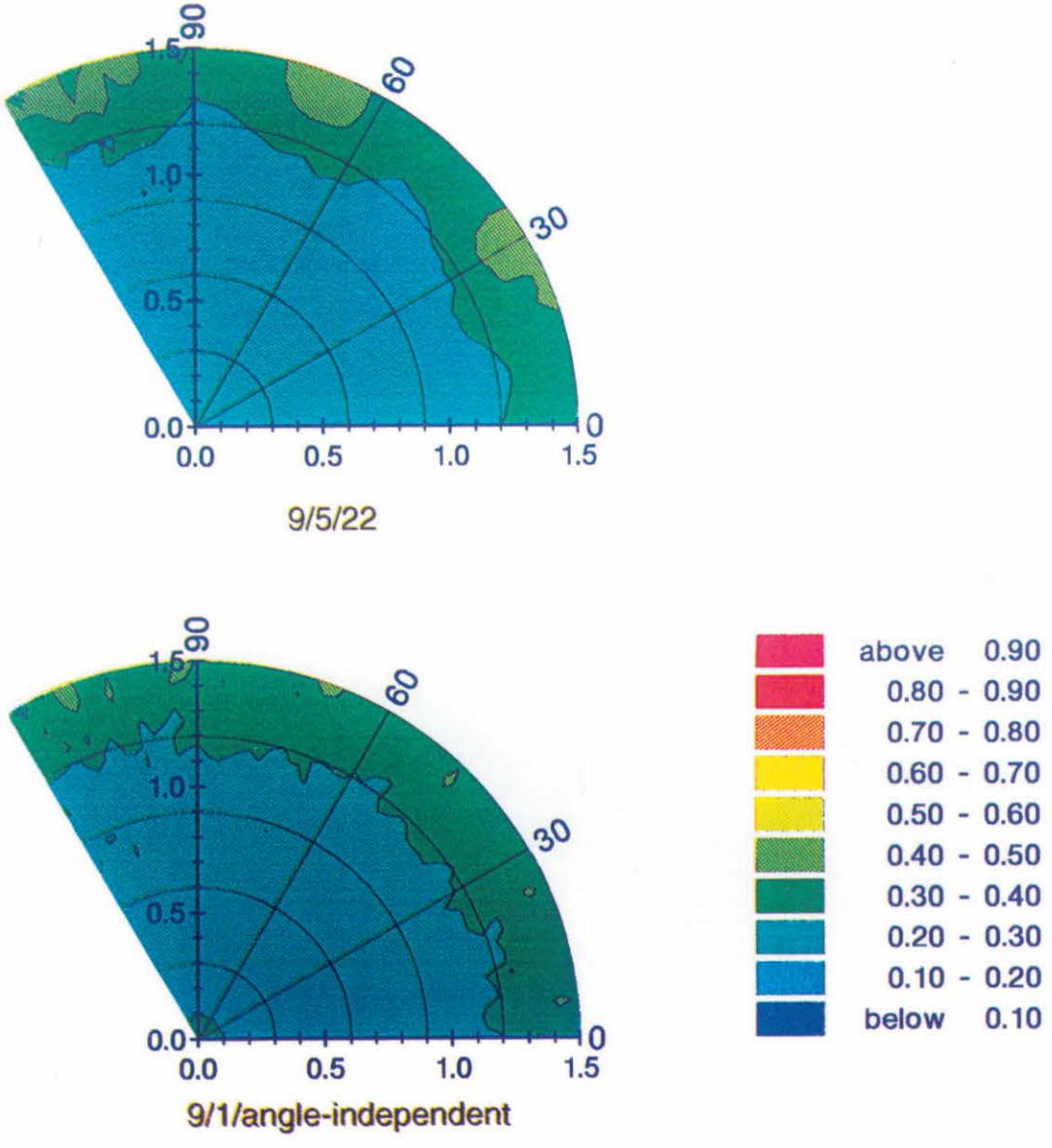

Figure 19. Nine Orifice Modules' Mixture Fraction Contours at z/R=1.0

REPORT DOCUMENTATION PAGE

Form Approved
OMB No. 0704-0188

1. AGENCY USE ONLY (*Leave blank*)	2. REPORT DATE	3. REPORT TYPE AND DATES COVERED
	January 1994	Technical Memorandum

4. TITLE AND SUBTITLE

Optimization of Orifice Geometry for Cross-Flow Mixing in a Cylindrical Duct

5. FUNDING NUMBERS

WU–537–02–20–00

6. AUTHOR(S)

W.A. Sowa, J.T. Kroll, G.S. Samuelsen, and J.D. Holdeman

7. PERFORMING ORGANIZATION NAME(S) AND ADDRESS(ES)

National Aeronautics and Space Administration
Lewis Research Center
Cleveland, Ohio 44135–3191

8. PERFORMING ORGANIZATION REPORT NUMBER

E–8278

9. SPONSORING/MONITORING AGENCY NAME(S) AND ADDRESS(ES)

National Aeronautics and Space Administration
Washington, DC 20546–0001

10. SPONSORING/MONITORING AGENCY REPORT NUMBER

NASA TM–106436
AIAA–94–0219

11. SUPPLEMENTARY NOTES

Prepared for the 32nd Aerospace Sciences Meeting and Exhibit, sponsored by the American Institute of Aeronautics and Astronautics, Reno, Nevada, January 10–13, 1994. W.A. Sowa, J.T. Kroll, and G.S. Samuelsen, UCI Combustion Laboratory, University of California, Irvine, California 92717, and J.D. Holdeman, NASA Lewis Research Center. Responsible person, J.D. Holdeman, (216) 433–5846.

12a. DISTRIBUTION/AVAILABILITY STATEMENT

Unclassified - Unlimited
Subject Category: 07

Available electronically at http://gltrs.grc.nasa.gov/GLTRS
This publication is available from the NASA Center for AeroSpace Information, (301) 621–0390.

12b. DISTRIBUTION CODE

13. ABSTRACT ***(Maximum 200 words)***

Mixing of gaseous jets in a cross-flow has significant applications in engineering, one example of which is the dilution zone of a gas turbine combustor. Despite years of study, the design of jet injection in combustors is largely based on practical experience. A series of experiments was undertaken to delineate the optimal mixer orifice geometry. A cross-flow to core-flow momentum-flux ratio of 40 and a mass flow ratio of 2.5 were selected as representative of an advanced design. An experimental test matrix was designed around three variables: the number of orifices, the orifice aspect ratio (long-to-short dimension), and the orifice angle. A regression analysis was performed on the data to arrive at an interpolating equation that predicted the mixing performance of orifice geometry combinations within the range of the test matrix parameters. Results indicate that mixture uniformity is a non-linear function of the number of orifices, the orifice aspect ratio, and the orifice angle. Optimum mixing occurs when the asymptotic mean jet trajectories are in the range of $0.35 < r/R < 0.5$ (where $r = 0$ is at the mixer wall) at $z/R = 1.0$. At the optimum number of orifices, the difference between shallow-angled slots with large aspect ratios and round holes is minimal and either approach will lead to good mixing performance. At the optimum number of orifices, it appears possible to have two local optimums where one corresponds to an aspect ratio of 1.0 and the other to a high aspect ratio.

14. SUBJECT TERMS	15. NUMBER OF PAGES
Dilution; CAW; Emissions; Jet mixing flow; Gas turbines; Combustion chamber	33
	16. PRICE CODE: A03

17. SECURITY CLASSIFICATION OF REPORT	18. SECURITY CLASSIFICATION OF THIS PAGE	19. SECURITY CLASSIFICATION OF ABSTRACT	20. LIMITATION OF ABSTRACT
Unclassified	Unclassified	Unclassified	

National Aeronautics and
Space Administration

Lewis Research Center
21000 Brookpark Rd.
Cleveland, OH 44135-3191